

# Geophysical Research Letters<sup>®</sup>



## RESEARCH LETTER

10.1029/2024GL113188

## Direct Evidence for Electron Pitch Angle Scattering Driven by Electrostatic Cyclotron Harmonic Waves

### Key Points:

- A decrease in electron fluxes is observed near the loss cone associated with an enhanced Electrostatic Cyclotron Harmonic (ECH) wave activity
- Energy-pitch angle dependent flux decrease is consistent with the prediction by the quasi-linear diffusion theory
- The first direct observation showing that ECH waves are capable of energy-dependent scattering of electrons near the loss cone

S. Kurita<sup>1</sup> , Y. Miyoshi<sup>2</sup> , S. Kasahara<sup>3</sup> , S. Yokota<sup>4</sup> , Y. Kasahara<sup>5</sup> , S. Matsuda<sup>5</sup> , A. Kumamoto<sup>6</sup> , F. Tsuchiya<sup>6</sup> , A. Matsuoka<sup>7</sup> , T. Hori<sup>2</sup> , K. Keika<sup>3</sup> , M. Teramoto<sup>8</sup> , K. Yamamoto<sup>2</sup> , and I. Shinohara<sup>9</sup> 

<sup>1</sup>Research Institute for Sustainable Humanosphere, Kyoto University, Uji, Japan, <sup>2</sup>Institute for Space-Earth Environmental Research, Nagoya University, Nagoya, Japan, <sup>3</sup>Department of Earth and Planetary Science, School of Science, The University of Tokyo, Tokyo, Japan, <sup>4</sup>Department of Earth and Space Science, Graduate School of Science, Osaka University, Toyonaka, Japan, <sup>5</sup>Graduate School of Natural Science and Technology, Kanazawa University, Kanazawa, Japan, <sup>6</sup>Graduate School of Science, Tohoku University, Sendai, Japan, <sup>7</sup>Graduate School of Science, Kyoto University, Kyoto, Japan, <sup>8</sup>Kyushu Institute of Technology, Iizuka, Japan, <sup>9</sup>Institute of Space and Astronautical Science, Japan Aerospace Exploration Agency, Sagami, Japan

### Correspondence to:

S. Kurita,  
kurita.satoshi.8x@kyoto-u.ac.jp

### Citation:

Kurita, S., Miyoshi, Y., Kasahara, S., Yokota, S., Kasahara, Y., Matsuda, S., et al. (2025). Direct evidence for electron pitch angle scattering driven by electrostatic cyclotron harmonic waves. *Geophysical Research Letters*, 52, e2024GL113188. <https://doi.org/10.1029/2024GL113188>

Received 20 OCT 2024

Accepted 1 FEB 2025

**Abstract** Electrostatic Cyclotron Harmonic (ECH) waves have been considered a potential cause of pitch angle scattering of electrons in the energy range from a few hundred eV to tens of keV. Theoretical studies have suggested that scattering by ECH waves is enhanced at lower pitch angles near the loss cone. Due to the insufficient angular resolution of particle detectors, it has been a great challenge to reveal ECH-driven scattering based on electron measurements. This study reports on variations in electron pitch angle distributions associated with ECH wave activity observed by the Arase satellite. The variation is characterized by a decrease in fluxes near the loss cone, and energy and pitch angle dependence of the flux decrease is consistent with the region of enhanced pitch angle scattering rates predicted by the quasi-linear diffusion theory. This study provides direct evidence for energy-pitch angle dependence of pitch angle scattering driven by ECH waves.

**Plain Language Summary** Near-Earth space is surrounded by the ionized gas so-called “plasma,” which is trapped by the Earth’s intrinsic magnetic field, forming the magnetosphere of the Earth. A variety of waves are present in the plasma, and interaction between plasma and waves results in acceleration, transport, and loss of plasma in the Earth’s magnetosphere. Electrostatic Cyclotron Harmonic (ECH) waves are one of the intense waves present in the magnetosphere. The waves are one candidate causing electron heating and loss of electrons in that region. Theoretical studies suggest that ECH waves contribute to a change in electron pitch angle, the angle between the velocity vector of electrons and the magnetic field, in the energy range from a few hundred electron volts to several tens of kilo-electron-volts. This process causes electron precipitation into the Earth’s atmosphere, resulting in permanent loss of electrons from the magnetosphere. Here, based on the observation by the Arase satellite together with a theoretical framework, we show the observational evidence that ECH waves can cause significant pitch angle changes of electrons in the energy range of 7–20 keV. This study strongly suggests that ECH waves contribute to electron dynamics in the inner magnetosphere through wave-particle interactions.

## 1. Introduction

Electrostatic Cyclotron Harmonic (ECH) waves are electrostatic emissions observed in bands between the harmonics of electron gyrofrequency  $f_{ce}$  (e.g., Hubbard & Birmingham, 1978; Kennel et al., 1970; Meredith et al., 2009). The waves appear outside the plasmopause and near the magnetic equator (e.g., Kazama et al., 2018; Meredith et al., 2009). Theoretical studies suggest that ECH waves are excited by loss-cone distributions of anisotropic hot electrons with cold plasma populations (Ashour-Abdalla & Kennel, 1978; Hubbard & Birmingham, 1978).

The first report on ECH waves observed by OGO-5 showed that the ECH waves had large wave amplitudes, typically between 1 and 10 mV/m, and the amplitude sometimes reached above 100 mV/m (Kennel et al., 1970). Evaluation of electron pitch angle diffusion rates suggests that the ECH waves are capable of rapid pitch angle scattering of a few keV electrons near the loss cone (Lyons, 1974) and indicated that ECH waves were responsible for the formation of “pancake” distributions, which is characterized by highly anisotropic pitch angle distributions

© 2025. The Author(s).

This is an open access article under the terms of the [Creative Commons Attribution License](https://creativecommons.org/licenses/by/4.0/), which permits use, distribution and reproduction in any medium, provided the original work is properly cited.

peaked at  $90^\circ$  (Wrenn et al., 1979). Belmont et al. (1983) subsequently showed that the amplitudes of ECH waves observed by GEOS-2 rarely exceeded 1 mV/m. Horne and Thorne (2000) extensively evaluated pitch angle diffusion rates by ECH waves and found that efficient pitch angle scattering was expected if the waves are present in an appropriate frequency range. Recent modeling studies concluded that whistler mode waves rather than ECH waves dominantly contribute to electron scattering in the velocity space in the inner magnetosphere because scattering rates by whistler mode waves were at least an order of magnitude greater than those by ECH waves (Thorne et al., 2010).

While scattering by ECH waves has been extensively investigated from the theoretical aspect, the theoretical studies have yet to be followed well by observational studies. Meredith et al. (1999) examined whether ECH waves and whistler mode waves could contribute to the formation of the “pancake” distributions using the CRRES satellite data. They compared the velocity distribution functions to the diffusion curve of whistler mode waves, which indicates a marginally stable state of velocity distribution functions after interactions between electrons and whistler mode waves (Gendrin, 1981; Summers et al., 1998). They found that the shape of velocity distribution functions was characterized well by the diffusion curve outside  $L = 6$ . In contrast, significant deviations of velocity distribution functions from the diffusion curves were identified inside  $L = 6$ . They suggested that ECH waves are mainly responsible for the formation of the “pancake” distribution at the lower L-shell.

The analysis by Meredith et al. (1999) cannot distinguish the region where efficient pitch angle scattering by ECH waves is operated since an overall shape of electron distribution functions is compared with the diffusion curve. Kurita et al. (2014) compared the shape of the velocity distribution functions with the diffusion curve in detail and showed that the shape of velocity distribution functions deviated from the diffusion curve at a low pitch angle near the loss cone (approximately below  $20^\circ$ ) in association with enhanced ECH wave activity, suggesting that the ECH waves scattered electrons at lower pitch angles near the loss cone. However, the energy and pitch angle dependent electron pitch angle scattering, which is predicted by the quasi-linear diffusion theory, is not revealed in Kurita et al. (2014).

These observational studies did not reveal the energy and pitch angle dependence of pitch angle scattering by ECH waves expected from the theoretical studies, which may be related to the instrument performance such as insufficient angular resolution and detection efficiency of electrons. It is possible that changes in electron pitch angle distributions due to ECH waves is revealed by measurement of electrons with good energy-angular resolution and high detection efficiency to capture faint changes in electron velocity distribution functions caused by wave-particle interactions. Medium Energy Particle experiments-electron analyzer (MEP-e, S. Kasahara, Yokota, Mitani, et al., 2018) onboard the Arase satellite (Miyoshi, Shinohara, et al., 2018), which measures electrons in the energy range from 7 to 87 keV, has a potential to accomplish the requirements. MEP-e measures electrons with the angular resolution of  $3.5^\circ$  and has the electron detection efficiency close to unity (S. Kasahara, Yokota, Mitani, et al., 2018). These features make it possible to observe electron fluxes inside the loss cone even in the magnetic equator (S. Kasahara, Yokota, Hori, et al., 2018) and to reveal rapid change in electron pitch angle distribution through interaction between electrons and chorus waves (Kurita et al., 2018).

Using the data obtained by MEP-e, Plasma Wave Experiment (Y. Kasahara, Kasaba, et al., 2018; Y. Kasahara, Kojima, et al., 2018), and Magnetic field experiment (Matsuoka, Teramoto, Imajo, et al., 2018; Matsuoka, Teramoto, Nomura, et al., 2018) onboard the Arase satellite, this paper reports on variation in electron fluxes associated with localized ECH activity which shows the dependence of flux decrease on energy and pitch angle. The dependence is consistent with quasi-linear pitch angle scattering rates by ECH waves.

## 2. Observation

The observation shown in this paper was made when the Arase satellite traversed its apogee and eventually encountered an energetic electron injection near the magnetic equator on 27 March 2017. Figures 1a–1d show an overview of plasma wave and electron data measured by PWE and MEP-e, respectively.

Figure 1a represents the frequency-time spectrogram of wave electric fields measured by High-Frequency Analyzer (HFA, Kumamoto et al., 2018) covering the frequency range from 10 to 400 kHz. The narrow band emission observed in the HFA frequency range (10–400 kHz) is the upper hybrid resonance (UHR) emission. The highly variable UHR frequency corresponds to the density variation at the satellite location.

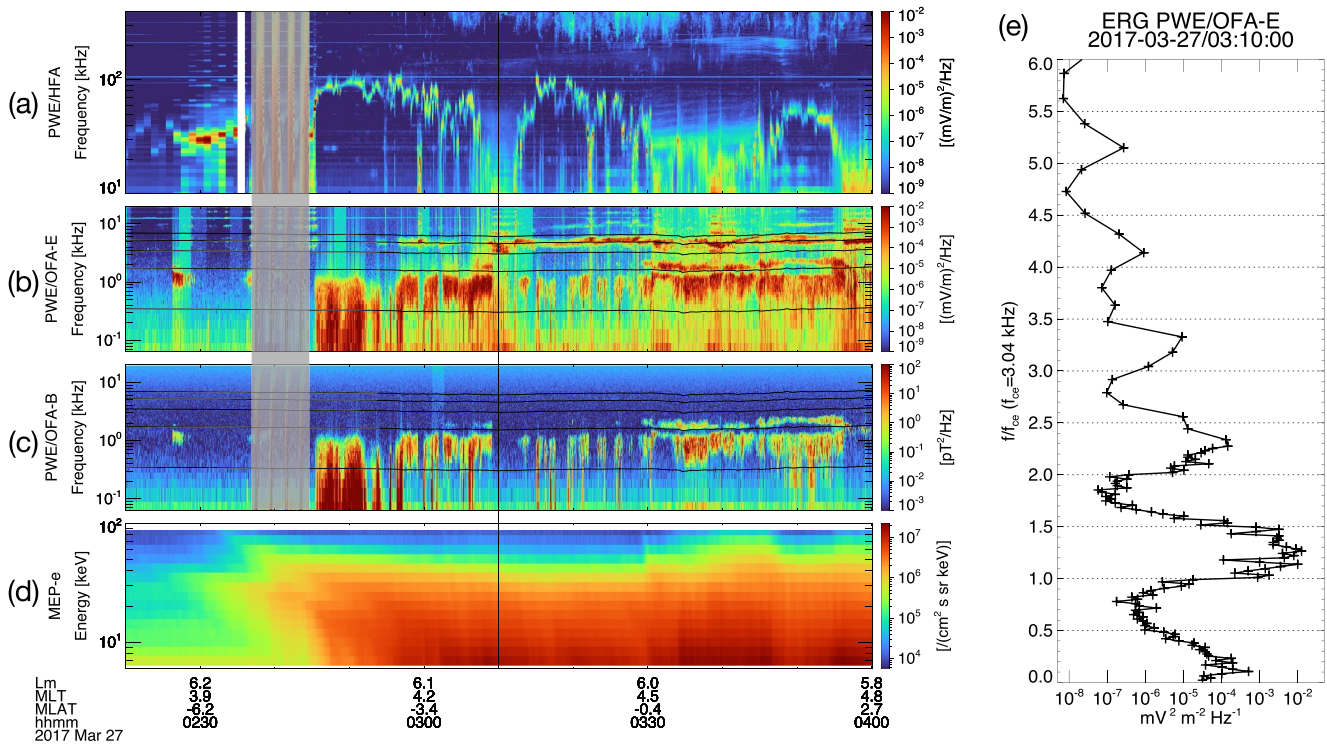


**Figure 1.** (a) Frequency-time spectrogram of wave electric fields in the frequency range from 10 to 400 kHz measured by HFA. (b, c) Frequency-time spectrogram of wave electric and magnetic fields in the frequency range from 0.1 to 20 kHz measured by OFA, respectively. (d) Energy-time spectrogram of electrons in the energy range from 7 to 80 keV observed by MEP-e. (e) Wave electric field power measured by OFA as a function of wave frequency normalized by the electron cyclotron frequency at 03:10:00 UT. The timing is indicated by the vertical line in (a–d).

Figures 1b and 1c show frequency-time spectra of wave electric and magnetic fields in the frequency range from 0.1 to 20 kHz computed by Onboard Frequency Analyzer (OFA, Matsuda et al., 2018) using signals from the wire probe antennas (Kasaba et al., 2017) and magnetic search coils (Ozaki et al., 2018), respectively. The local electron cyclotron frequency,  $f_{ce}$ , is computed from the MGF measurement, and magenta lines in Figures 1b and 1c represent 0.1, 0.5, 1, 1.5, and 2 times of  $f_{ce}$ . Whistler-mode waves were observed below  $f_{ce}$  after ~0240 UT, and intense ECH waves appeared after ~0252 UT in bands between the harmonics of  $f_{ce}$ . The highest frequency band of the ECH waves varied in time, while the most intense wave power was located between  $f_{ce}$  and  $2f_{ce}$ . These wave activities were not strongly correlated with the density variations inferred from the UHR frequency variation.

Figure 1d shows an energy-time spectrogram of spin-averaged electron fluxes measured by MEP-e in the energy range from 7 to 80 keV. The MEP-e measurement indicates the electron flux enhancement with an energy-time dispersed signature around 0240 UT. The beginning of enhanced wave activity was associated well with the appearance of the energetic electron injections, indicating that the injected electrons would be responsible for the excitation of the waves. However, the variation in electron fluxes was smooth compared to the plasma wave intensity variation. It is difficult to investigate the signature of change in electron distribution functions from these time-series plots.

The analysis reported in this paper focused on the time interval when intense ECH waves appeared with very weak or no whistler mode wave activity around 0310 UT as indicated by the vertical line in Figures 1a–1d. The wave electric field power on 0310 UT is shown in Figure 1e. The most intense ECH wave power during this period is in the frequency range from 1 to  $1.5f_{ce}$ . The bandwidth of this ECH wave is relatively broad compared to ECH waves observed during the other periods, as seen in Figure 1b.

The magnified view of wave activities and electron pitch angle distributions are shown in Figure 2. Figure 2a shows the frequency-time spectrogram of wave electric field power computed by PWE/OFA. Figures 2b–2j show pitch angle distributions of electrons in the energy range from 7.0 to 29.3 keV observed by MEP-e. The pitch

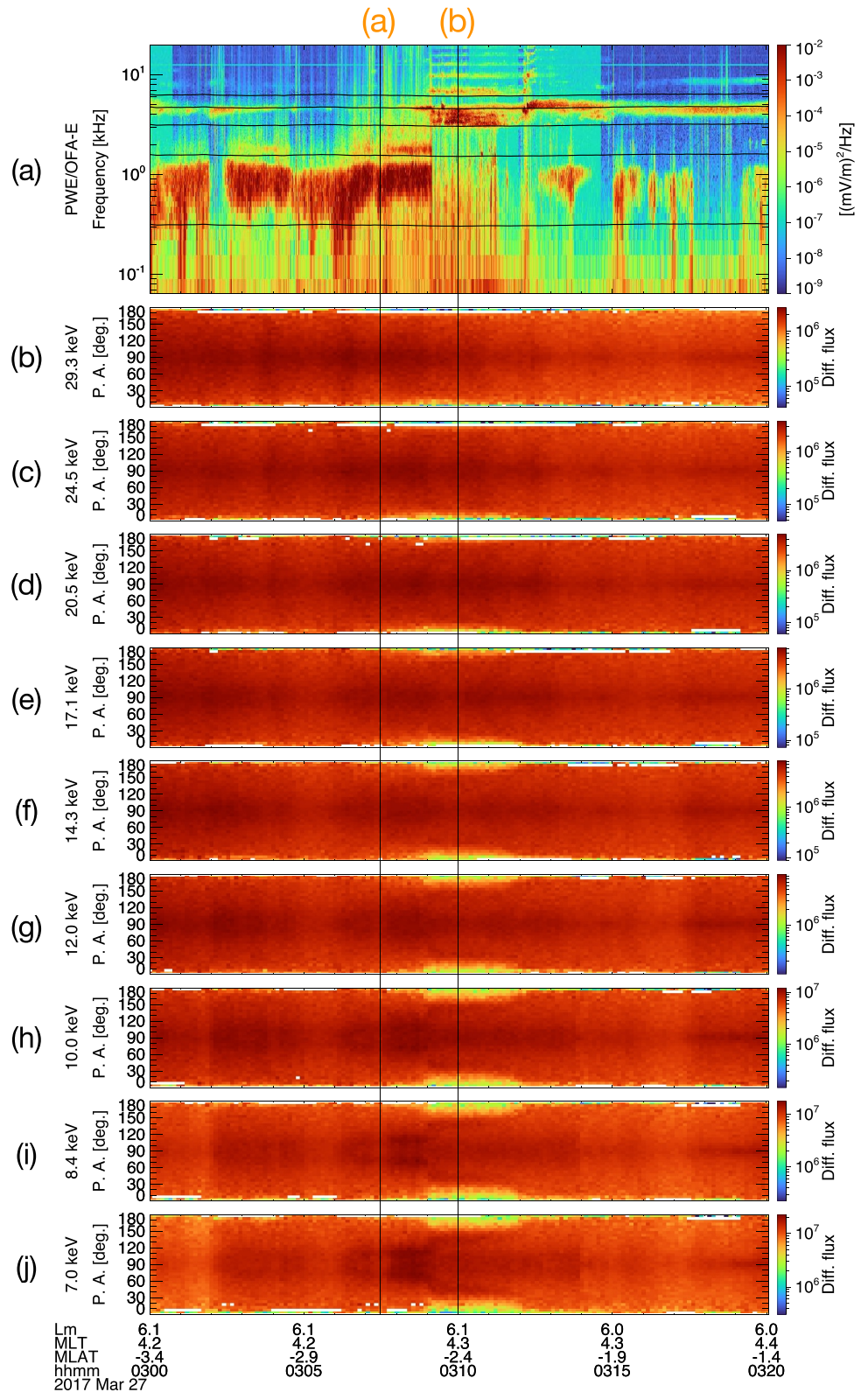


**Figure 2.** (a) Frequency-time spectrogram of wave electric fields computed by OFA. The five magenta lines represent 0.1, 0.5, 1, 1.5, and 2 times of electron cyclotron frequency, respectively. (b–j) Electron pitch angle distributions observed by MEP-e in the energy range from 7.0 to 29.3 keV. The two vertical lines indicate the timing when the distributions shown in Figure 3 are obtained.

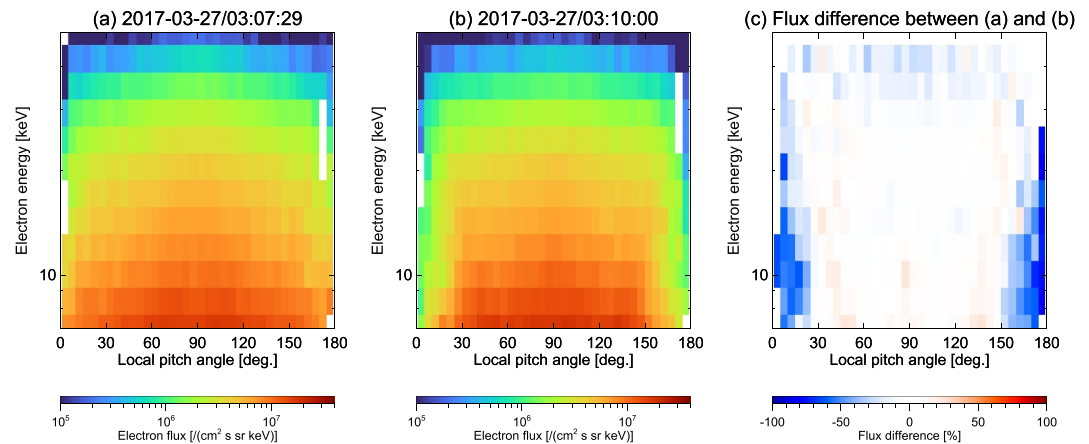


**Figure 3.** Electron fluxes as a function of local pitch angle and energy observed by MEP-e (a) before and (b) during the enhancement of ECH wave activity. (c) Flux difference between (a, b) in unit of % as a function of local pitch angle and energy. The absolute flux difference is normalized by initial distribution. Negative values indicate decrease in electron fluxes compared to (a).

angle distribution of 7.0 keV electrons shows the decrease in electron fluxes at low ( $<30^\circ$ ) pitch angles, which is accompanied well by the appearance of the ECH waves. A significant decrease in electron fluxes at low pitch angles can be seen in the electron energy range from 7.0 to 14.3 keV, while the flux depression at low pitch angles is less evident for 17.1 and 20.5 keV electrons. The pitch angle distributions of 24.5 and 29.3 keV electrons do not show clear changes associated with the enhanced ECH wave activity.

The electron distribution functions before and during the ECH wave activity are shown in Figures 3a and 3b. The timings when these distributions are obtained are indicated by the vertical lines in Figure 2. Before the ECH wave activity, when the distribution shown in Figure 3a is acquired, intense whistler-mode waves are intermittently observed. We examined the variations in electron fluxes in the energy range from 7.0 to 29.3 keV integrated over the pitch angle range of  $5\text{--}30^\circ$  to rule out the possibility that the absence of the whistler-mode wave activity results in the observed change in the electron pitch angle distributions at low pitch angle range associated with the ECH wave activity. We find that the correlation between the whistler-mode wave intensity and the 7.0–29.3 keV electron fluxes is quite low (not shown), indicating that the distribution shown in Figure 3a can be assumed to be the initial distribution before pitch angle scattering by the ECH waves operates, and that the observed change in the pitch angle distribution associated with the ECH wave activity (Figure 3b) is dominated by pitch angle scattering by the ECH waves rather than the absence of the whistler-mode wave activity. It is noted that this analysis relies on the assumption that the whistler-mode wave activity does not significantly modify the electron pitch angle distributions at the low pitch angle range during the time interval of interest. Even though we find the low correlation between the whistler-mode wave activity and the electron flux in the pitch angle range of  $5\text{--}30^\circ$ , a flux decrease would be caused by the sudden reduction of whistler-mode wave activity. Thus, the flux decrease shown in Figure 3b might be overestimated if we assume that the flux decrease is purely caused by pitch angle scattering due to the ECH waves.

The flux difference between the distributions is shown in Figure 3c to emphasize the change in the distributions in association with the ECH wave activity. The flux difference is normalized by initial distribution, and the energy-pitch angle bins with an average count above 10 are shown. Negative values in Figure 3c indicate the decrease in electron fluxes compared to the initial distribution. The energy-pitch angle-dependent flux decrease can be seen near the loss cone (pitch angle range of  $0\text{--}30^\circ$  and  $150\text{--}180^\circ$ ) in the energy range below 20 keV. As the electron energy increases above 20 keV, the decrease in fluxes near the loss cone is less evident. The region and flux decrease dependency are consistent with enhanced pitch angle scattering rates predicted by quasi-linear diffusion theory (e.g., Ni et al., 2012).

### 3. Evaluation of Pitch Angle Scattering Rate From the Observed Pitch Angle Distribution

The significant advantage of MEP-e is the fine angular resolution, which enables us to resolve electron fluxes inside and outside the loss cone (S. Kasahara, Yokota, Hori, et al., 2018). Utilizing this angular resolution, it is possible to evaluate pitch angle scattering rates near the loss cone by comparing the measured pitch angle distributions near the loss cone with theoretically derived ones.

Fokker-Planck equations for particle diffusion give the following equilibrium pitch angle distributions inside and outside the loss cone (Kennel & Petschek, 1966; Theodoridis & Paolini, 1967)

$$J_{\text{in}}(\alpha_{\text{eq,in}}, E) = \frac{S(E)}{D^*} \left\{ \frac{I_0\left(\frac{\alpha_{\text{eq,in}}}{\alpha_0} z_0\right)}{z_0 I_1(z_0)} \right\}, \quad (1)$$

$$J_{\text{out}}(\alpha_{\text{eq,out}}, E) = \frac{S(E)}{D^*} \left\{ \frac{I_0(z_0)}{z_0 I_1(z_0)} + \ln \frac{\sin \alpha_{\text{eq,out}}}{\sin \alpha_0} \right\}, \quad (2)$$

where  $S(E)$  is the particle rate entering the loss cone,  $z_0 = \frac{\alpha_0}{\sqrt{\tau D^*}}$ ,  $D^*$  near the loss cone is approximately equal to  $D^* \approx D_{\alpha\alpha}(E)|_{\alpha=\alpha_0} \times \cos(\alpha_0)$ , where  $D_{\alpha\alpha}(E)|_{\alpha=\alpha_0}$  is the bounce-averaged electron pitch angle diffusion coefficient at the equatorial loss cone  $\alpha = \alpha_0$ .  $\alpha_{\text{eq,in}}$  and  $\alpha_{\text{eq,out}}$  are the equatorial electron pitch angles inside and outside the loss cone, respectively.  $E$  and  $\tau$  are the electron kinetic energy and the quarter of the electron bounce period.  $I_0$  and  $I_1$  are the modified Bessel functions. As the electron pitch angle diffusion coefficient increases, electron pitch angle distributions inside the loss cone become flat (Figure 1a of Li et al., 2013). It is possible to evaluate the pitch angle diffusion coefficient near the loss cone by comparing the electron pitch angle distribution near the loss cone measured by MEP-e with that derived from Equations 1 and 2 by varying  $D^*$  with respect to the strong diffusion limit  $D_{\text{SD}} = \frac{1}{4}\tau$  (Kennel, 1969). We note that, to compare the MEP-e observation with the theoretical one, the pitch angle distribution obtained from Equations 1 and 2 are convolved with the angular response of MEP-e, which is characterized by the Gaussian distribution with a full-width-half maximum of  $3.5^\circ$  (S. Kasahara, Yokota, Mitani, et al., 2018; S. Kasahara, Yokota, Hori, et al., 2018). We adjusted  $S(E)$  so that  $J_{\text{out}}$  matches measured electron flux at  $\alpha_{\text{eq,out}} = 13.5^\circ$ .

Figure 4 shows the pitch angle distributions around the loss cone derived from the MEP-e measurement, averaged over a 1.5-min (03:09:40–03:11:10 UT) and a 1-degree pitch angle interval. Black asterisk symbols and vertical bars are the averaged electron flux and standard deviation, respectively. Small dots are individual measurements of MEP-e for the 1.5-min interval. Color-coded dashed lines are the theoretical pitch angle distributions (Equations 1 and 2), which are convolved with the angular response of MEP-e. We consider four levels of pitch angle diffusion rates relative to the strong diffusion limit. For 7 keV electrons, the measured pitch angle distribution is close to the theoretical one with  $D^* = D_{\text{sd}}$ , indicating that these electrons are expected to experience intense pitch angle scattering at a rate close to the strong diffusion limit. For higher energy electrons (14.3 and 20.5 keV), the measured pitch angle distributions are close to theoretical ones, with the diffusion rate lower than the strong diffusion limit. These energy-dependent pitch angle diffusion rates evaluated from the pitch angle distributions are qualitatively consistent with the theoretical prediction that the pitch angle diffusion rate of ECH waves tends to be smaller for higher energy electrons.

### 4. Discussion and Summary

The importance of pitch angle scattering by ECH waves has been discussed for decades based on the survey of ECH wave intensity (Kennel et al., 1970; Belmont et al., 1983; Meredith et al., 2009; Ni et al., 2011) and modeling works using the quasi-linear diffusion theory (Lyons, 1974; Horne & Thorne, 2000; Ni et al., 2012). The modeling works have led the discussion quantitatively by evaluating pitch angle scattering rates by ECH waves. A few studies use electron measurements to investigate the effects of ECH waves on electron pitch angle scattering. Meredith et al. (1999) and Kurita et al. (2014) used electron measurements to find the change in electron distribution functions associated with ECH wave activity. To figure out the slight change in electron distribution

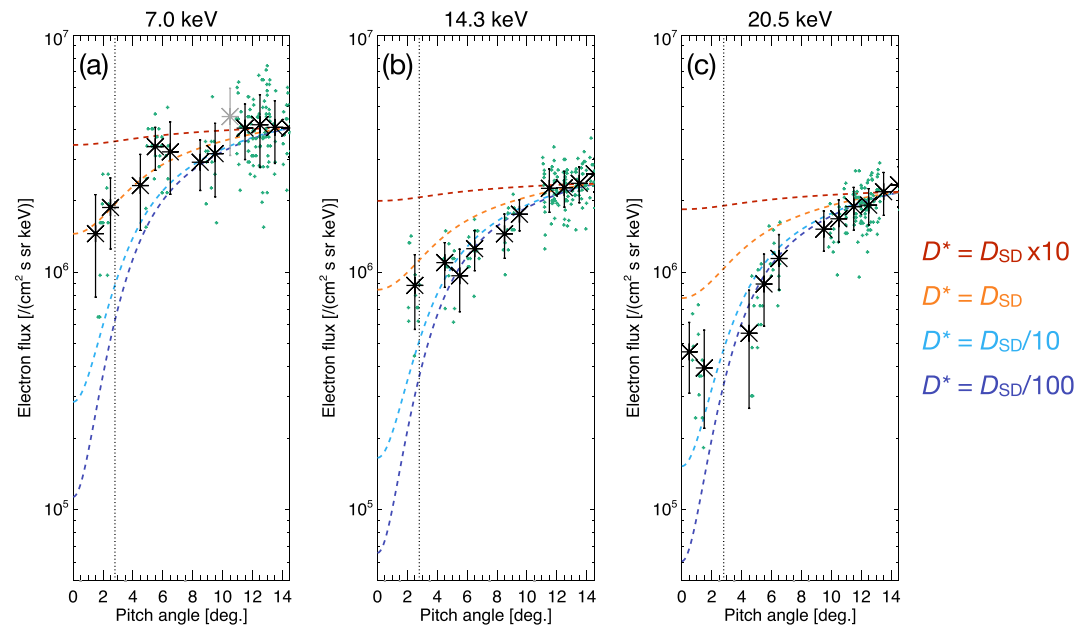


**Figure 4.** Electron pitch angle distributions around the loss cone obtained from the MEP-e measurement for three energy channels and theoretically derived pitch angle distributions, which are convolved with the angular response of MEP-e to reproduce the MEP-e measurement. Black asterisk symbols represent the averaged electron fluxes at every 1-degree interval, computed from the individual measurement obtained for 1.5 min and denoted by the small symbols. Black vertical bars indicate the standard deviation of the averaged flux. When the averaged electron flux is computed from the number of individual measurements less than 4, the flux is denoted by the gray asterisk. Four theoretical pitch angle distributions with different pitch angle diffusion rates  $D^*$  are represented by the dashed lines with different colors. The vertical dotted line in each figure represents the loss cone angle at the satellite location.

functions by ECH wave-driven scattering, these studies used the theoretical reference of the so-called diffusion curve, which shows a marginally stable state after the interaction between electrons and waves (Gendrin, 1981; Summers et al., 1998). However, these studies cannot address the energy and pitch angle-dependent pitch angle scattering by ECH waves predicted by the quasi-linear diffusion theory. Fukizawa et al. (2020) performed an event analysis of the correlation between the electron fluxes inside the loss cone and ECH wave intensity together with the evaluation of the pitch angle diffusion rates by the ECH waves with several assumptions, suggesting that the ECH waves are responsible for pitch angle scattering of electrons into the loss cone during the event. Statistical investigation of the loss cone filling by ECH waves is performed by Fukizawa et al. (2022), showing that ECH waves have the potential to cause intense electron pitch angle scattering, which leads to filling the loss cone. The investigation performed by Fukizawa et al. (2020, 2022) concentrated on whether ECH waves can scatter a significant amount of electrons into the loss cone, while the change in the electron pitch angle distributions by ECH waves is not clarified. This study unveils the change in electron pitch angle distributions accompanied by the ECH wave activity, which depends on the energy and pitch angle. Furthermore, from the analysis of the electron pitch angle distributions near the loss cone, we qualitatively show that pitch angle diffusion rates by the ECH waves near the loss cone are energy-dependent.

It should be noted that intense ECH waves appear without any significant change in electron pitch angle distributions observed by MEP-e during the time interval shown in Figure 2. For example, the amplitude of the ECH wave between  $f_{ce}$  and  $2 f_{ce}$  ranges from 10 to 50 mV/m around 0310 UT, while the ECH wave in the same frequency range around  $\sim 0312$  UT has a wave amplitude exceeding 100 mV/m. The electric field measurement is calibrated by considering the antenna impedance in a vacuum and the effective antenna length of  $\sim 15$  m (Matsuda et al., 2021). The comparison of the wave amplitude suggests that large amplitude ECH waves do not necessarily contribute to efficient pitch angle scattering of tens keV electrons. The difference between these two ECH waves is the wave frequency range and bandwidth. The frequency of the ECH wave that contributes to electron pitch angle scattering lies between  $f_{ce}$  and  $1.5 f_{ce}$ . The frequency bandwidth of the ECH wave is wider compared to ECH waves during the other time interval. It is suggested that the frequency distribution of ECH wave power is an

important controlling factor in causing efficient pitch angle scattering of energetic electrons through resonance conditions with electrons.

It is now widely accepted that whistler mode chorus waves mainly contribute to the formation of the “pancake” distributions of electrons in the energy range from several to a few tens of keV during their convective transport from the magnetotail to the dayside magnetosphere (Tao et al., 2011; Thorne et al., 2010), which indicates that overall shape of the distribution function is mainly determined by resonant interaction between the electrons and whistler-mode chorus waves. On the other hand, as demonstrated observationally for the first time in this study, the pitch angle scattering of electrons by ECH waves in the pitch angle range near the loss cone is energy dependent. Detecting faint flux changes near the loss cone by particle instruments onboard past satellite missions is challenging because of insufficient angular resolution and detection efficiency. Combining the high-quality data set obtained by MEP-e and the pitch angle distribution predicted by the quasi-linear diffusion theory, the electron pitch angle scattering rate by ECH waves near the loss cone can be evaluated experimentally and statistically. This analysis gives new insights into the contribution of ECH waves to electron dynamics through wave-particle interactions, which is left to be our future work.

### Data Availability Statement

The Science data of the ERG (Arase) satellite used in this study were obtained from the ERG Science Center (Miyoshi, Hori, et al., 2018) operated by ISAS/JAXA and ISEE/Nagoya University (<https://ergsc.isee.nagoya-u.ac.jp/index.shtml.en>). The MEP-e Level 2 v1.01 (S. Kasahara, Yokota, Hori, et al., 2018) and MGF Level 2 v03.04 data (Matsuoka, Teramoto, Imajo, et al., 2018) were analyzed to generate the energy-time spectrogram and pitch angle distributions. The PWE/OFA-SPEC Level 2 v2.03 data (Y. Kasahara, Kojima, et al., 2018) was used to show the frequency-time spectrograms of electromagnetic fields. We also used the Level 2 v04 orbit data of the Arase satellite (Miyoshi, Shinohara, & Jun, 2018). The analysis performed in this study was conducted by using the SPEDAS software (<http://themis.ssl.berkeley.edu/software.shtml>, Angelopoulos et al., 2019) including ERG plug-in tools ([https://ergsc.isee.nagoya-u.ac.jp/erg\\_socware/erg\\_plugin/](https://ergsc.isee.nagoya-u.ac.jp/erg_socware/erg_plugin/)), which are publicly available and can be used without any restrictions.

### Acknowledgments

This study was supported by Grant-in-Aid for Scientific Research (15H05815, 15H05747, 16H06286, 16H04056, 17H06140, 19K03949, 20H01959, 21H04526, 22K03699, 22H00173, 22K21345, 22KK0046, 23K25925, 23H05429).

### References

- Angelopoulos, V., Cruce, P., Drozdov, A., Grimes, E. W., Hatzigeorgiu, N., King, D. A., et al. (2019). The Space Physics Environment Data Analysis System (SPEDAS). *Space Science Reviews*, 215(1), 9. <https://doi.org/10.1007/s11214-018-0576-4>
- Ashour-Abdalla, M., & Kennel, C. F. (1978). Nonconvective and convective electron cyclotron harmonic instabilities. *Journal of Geophysical Research*, 83(A4), 1531–1543. <https://doi.org/10.1029/JA083iA04p01531>
- Belmont, G., Fontaine, D., & Canu, P. (1983). Are equatorial electron cyclotron waves responsible for diffuse auroral electron precipitation? *Journal of Geophysical Research*, 88(A11), 9163–9170. <https://doi.org/10.1029/JA088iA11p09163>
- Fukizawa, M., Sakanoi, T., Miyoshi, Y., Kazama, Y., Katoh, Y., Kasahara, Y., et al. (2020). Pitch-angle scattering of inner magnetospheric electrons caused by ECH waves obtained with the Arase satellite. *Geophysical Research Letters*, 47(23), e2020GL089926. <https://doi.org/10.1029/2020GL089926>
- Fukizawa, M., Sakanoi, T., Miyoshi, Y., Kazama, Y., Katoh, Y., Kasahara, Y., et al. (2022). Statistical study of approaching strong diffusion of low-energy electrons by chorus and ECH waves based on *in situ* observations. *Journal of Geophysical Research: Space Physics*, 127(3), e2022JA030269. <https://doi.org/10.1029/2022JA030269>
- Gendrin, R. (1981). General relationships between wave amplification and particle diffusion in a magnetoplasma. *Reviews of Geophysics*, 19(1), 171–184. <https://doi.org/10.1029/RG019i001p00171>
- Horne, R. B., & Thorne, R. M. (2000). Electron pitch angle diffusion by electrostatic electron harmonic waves: The origin of pancake distributions. *Journal of Geophysical Research*, 105(A3), 5391–5402. <https://doi.org/10.1029/1999ja000447>
- Hubbard, R. F., & Birmingham, T. J. (1978). Electrostatic emissions between electron gyroharmonics in the outer magnetosphere. *Journal of Geophysical Research*, 83(A10), 4837–4850. <https://doi.org/10.1029/ja083ia10p04837>
- Kasaba, Y., Ishisaka, K., Kasahara, Y., Imachi, T., Yagitani, S., Kojima, H., et al. (2017). Wire Probe Antenna (WPT) and Electric Field Detector (EFD) of Plasma Wave Experiment (PWE) aboard the Arase satellite: Specifications and initial evaluation results. *Earth, Planets and Space*, 69(1), 174. <https://doi.org/10.1186/s40623-017-0760-x>
- Kasahara, S., Yokota, S., Hori, T., Keika, K., Miyoshi, Y., & Shinohara, I. (2018). The MEP-e instrument Level-2 3-D flux data of Exploration of energization and Radiation in Geospace (ERG) Arase satellite [Dataset]. <https://doi.org/10.34515/DATA.ERG-02000>
- Kasahara, S., Yokota, S., Mitani, T., Asamura, K., Hirahara, M., Shibano, Y., & Takashima, T. (2018). Medium-Energy Particle experiments-electron analyser (MEP-e) for the Exploration of energization and Radiation in Geospace (ERG) mission. *Earth Planets and Space*, 70(1), 69. <https://doi.org/10.1186/s40623-018-0847-z>
- Kasahara, Y., Kasaba, Y., Kojima, H., Yagitani, S., Ishisaka, K., Kumamoto, A., et al. (2018). The Plasma Wave Experiment (PWE) on board the Arase (ERG) satellite. *Earth Planets and Space*, 70(1), 86. <https://doi.org/10.1186/s40623-018-0842-4>
- Kasahara, Y., Kojima, H., Matsuda, S., Ozaki, M., Yagitani, S., Shoji, M., et al. (2018). The PWE/OFA instrument Level-2 power spectrum data of Exploration of energization and Radiation in Geospace (ERG) Arase satellite [Dataset]. <https://doi.org/10.34515/DATA.ERG-08000>

- Kazama, Y., Kojima, H., Miyoshi, Y., Kasahara, Y., Usui, H., Wang, B.-J., et al. (2018). Density depletions associated with enhancements of electron cyclotron harmonic emissions: An ERG observation. *Geophysical Research Letters*, *45*(19), 10075–10083. <https://doi.org/10.1029/2018GL080117>
- Kennel, C. F. (1969). Consequences of a magnetospheric plasma. *Reviews of Geophysics*, *7*(1–2), 379–419. <https://doi.org/10.1029/RG007i001p00379>
- Kennel, C. F., & Petschek, H. E. (1966). Limit on stably trapped particle fluxes. *Journal of Geophysical Research*, *71*(1), 1–28. <https://doi.org/10.1029/JZ071i001p00001>
- Kennel, C. F., Scarf, F. L., Fredricks, R. W., McGehee, J. H., & Coroniti, F. V. (1970). VLF electric field observations in the magnetosphere. *Journal of Geophysical Research*, *75*(31), 6136–6152. <https://doi.org/10.1029/ja075i031p06136>
- Kumamoto, A., Tsuchiya, F., Kasahara, Y., Kasaba, Y., Kojima, H., Yagitani, S., et al. (2018). High Frequency Analyzer (HFA) of Plasma Wave Experiment (PWE) onboard the Arase spacecraft. *Earth Planets and Space*, *70*(1), 82. <https://doi.org/10.1186/s40623-018-0854-0>
- Kurita, S., Miyoshi, Y., Cully, C. M., Angelopoulos, V., Contel, O. L., Hikishima, M., & Misawa, H. (2014). Observational evidence of electron pitch angle scattering driven by ECH waves. *Geophysical Research Letters*, *41*(22), 8076–8080. <https://doi.org/10.1002/2014GL061927>
- Kurita, S., Miyoshi, Y., Kasahara, S., Yokota, S., Kasahara, Y., Matsuda, S., et al. (2018). Deformation of electron pitch angle distributions caused by upper band chorus observed by the Arase satellite. *Geophysical Research Letters*, *45*(16), 7996–8004. <https://doi.org/10.1029/2018gl079104>
- Li, W., Ni, B., Thorne, R. M., Bortnik, J., Green, J. C., Kletzing, C. A., et al. (2013). Constructing the global distribution of chorus wave intensity using measurements of electrons by the POES satellites and waves by the Van Allen Probes. *Geophysical Research Letters*, *40*(17), 4526–4532. <https://doi.org/10.1002/grl.50920>
- Lyons, L. R. (1974). Electron diffusion driven by magnetospheric electrostatic waves. *Journal of Geophysical Research*, *79*(4), 575–580. <https://doi.org/10.1029/JA079i004p00575>
- Matsuda, S., Kasahara, Y., Kojima, H., Kasaba, Y., Yagitani, S., Ozaki, M., et al. (2018). Onboard software of plasma wave experiment aboard Arase: Instrument management and signal processing of waveform capture/onboard frequency analyzer. *Earth Planets and Space*, *70*(1), 75. <https://doi.org/10.1186/s40623-018-0838-0>
- Matsuda, S., Kojima, H., Kasahara, Y., Kasaba, Y., Kumamoto, A., Tsuchiya, F., et al. (2021). Direct antenna impedance measurement for quantitative AC electric field measurement by Arase. *Journal of Geophysical Research: Space Physics*, *126*(6), e2021JA029111. <https://doi.org/10.1029/2021JA029111>
- Matsuoka, A., Teramoto, M., Imajo, S., Kurita, S., Miyoshi, Y., & Shinohara, I. (2018). The MGF instrument Level-2 spin-averaged magnetic field data of Exploration of energization and Radiation in Geospace (ERG) Arase satellite [Dataset]. <https://doi.org/10.34515/DATA.ERG-06001>
- Matsuoka, A., Teramoto, M., Nomura, R., Nose, M., Fujimoto, A., Tanaka, Y., et al. (2018). The ARASE(ERG) magnetic field investigation. *Earth Planets and Space*, *70*(1), 43. <https://doi.org/10.1186/s40623-018-0800-1>
- Meredith, N. P., Horne, R. B., Thorne, R. M., & Anderson, R. R. (2009). Survey of upper band chorus and ECH waves: Implications for the diffuse aurora. *Journal of Geophysical Research*, *114*(A7), A07218. <https://doi.org/10.1029/2009JA014230>
- Meredith, N. P., Johnstone, A. D., Szita, S., Horne, R. B., & Anderson, R. R. (1999). “Pancake” electron distributions in the outer radiation belts. *Journal of Geophysical Research*, *104*(A6), 12431–12444. <https://doi.org/10.1029/1998ja900083>
- Miyoshi, Y., Hori, T., Shoji, M., Teramoto, M., Chang, T. F., Matsuda, S., et al. (2018). The ERG Science Center. *Earth Planets and Space*, *70*(1), 96. <https://doi.org/10.1186/s40623-018-0867-8>
- Miyoshi, Y., Shinohara, I., & Jun, C.-W. (2018). The Level-2 orbit data of Exploration of energization and Radiation in Geospace (ERG) Arase satellite [Dataset]. <https://doi.org/10.34515/DATA.ERG-12000>
- Miyoshi, Y., Shinohara, I., Takashima, T., Asamura, K., Higashio, N., Mitani, T., et al. (2018). Geospace Exploration Project ERG. *Earth Planets and Space*, *70*(1), 101. <https://doi.org/10.1186/s40623-018-0862-0>
- Ni, B., Liang, J., Thorne, R. M., Angelopoulos, V., Horne, R. B., Kubyskhina, M., et al. (2012). Efficient diffuse auroral electron scattering by electrostatic electron cyclotron harmonic waves in the outer magnetosphere: A detailed case study. *Journal of Geophysical Research*, *117*(A1), A01218. <https://doi.org/10.1029/2011ja017095>
- Ni, B., Thorne, R., Liang, J., Angelopoulos, V., Cully, C., Li, W., et al. (2011). Global distribution of electrostatic electron cyclotron harmonic waves observed on THEMIS. *Geophysical Research Letters*, *38*(17), L17105. <https://doi.org/10.1029/2011gl048793>
- Ozaki, M., Yagitani, S., Kasahara, Y., Kojima, H., Kasaba, Y., Kumamoto, A., et al. (2018). Magnetic Search Coil (MSC) of Plasma Wave Experiment (PWE) aboard the Arase (ERG) satellite. *Earth Planets and Space*, *70*(1), 76. <https://doi.org/10.1186/s40623-018-0837-1>
- Summers, D., Thorne, R. M., & Xiao, F. (1998). Relativistic theory of wave-particle resonant diffusion with application to electron acceleration in the magnetosphere. *Journal of Geophysical Research*, *103*(A9), 20487–20500. <https://doi.org/10.1029/98JA01740>
- Tao, X., Thorne, R. M., Li, W., Ni, B., Meredith, N. P., & Horne, R. B. (2011). Evolution of electron pitch angle distributions following injection from the plasma sheet. *Journal of Geophysical Research*, *116*(A4), A04229. <https://doi.org/10.1029/2010JA016245>
- Theodoridis, G. C., & Paolini, F. R. (1967). Pitch angle diffusion of relativistic outer belt electrons. *Annales Geophysicae*, *23*, 375–381.
- Thorne, R. M., Ni, B., Tao, X., Horne, R. B., & Meredith, N. P. (2010). Scattering by chorus waves as the dominant cause of diffuse auroral precipitation. *Nature*, *467*(7318), 943–946. <https://doi.org/10.1038/nature09467>
- Wrenn, G. L., Johnson, J. F. E., & Sojka, J. J. (1979). Stable “pancake” distributions of low energy electrons in the plasma trough. *Nature*, *279*(5713), 512–514. <https://doi.org/10.1038/279512a0>